Flow downstream of an aerator - aerator spacing

Ecoulement en aval d'un aérateur - disposition des aérateurs

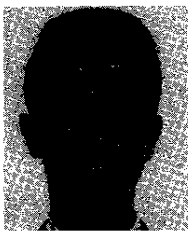

H. CHANSON
Engineering Consultant,
143, rue de la Pompe, 75116 Paris, France

SUMMARY
Cavitation erosion damage to spillway surfaces may be prevented with the use of aeration devices (aerators), introducing air in the layers close to the channel bottom.
A study of the flow downstream of a spillway aerator was performed on the Clyde dam spillway model. The results are presented and a comparison between the free-surface aeration and the flow downstream of an aerator is developed. Such a method enables to compute the flow parameters at any point downstream of an aerator, in particular the air concentration near the spillway bottom. The computed results are compared with experimental data.
This analysis contributes to a method for the determination of aerator spacing and aerator location.

RÉSUMÉ
Les dommages causés par l'érosion par cavitation sur les coursiers des évacuateurs de crues peuvent être empêchés à l'aide d'aérateurs, introduisant artificiellement de l'air dans l'écoulement proche de la surface des coursiers.
Une étude de l'écoulement en aval d'un aérateur a été menée sur le modèle de l'évacuateur de crues du barrage de Clyde. Les résultats sont présentés, et une comparaison entre l'entraînement d'air d'un écoulement à surface libre et l'écoulement en aval d'un aérateur est développée. Cette méthode permet de calculer en tout point les caractéristiques d'un écoulement en aval d'un aérateur, et en particulier la concentration en air près de la surface du coursier. Les calculs sont comparés avec les résultats expérimentaux.
Cette analyse développe une méthode permettant de déterminer la disposition optimale des aérateurs sur un coursier.

1 Introduction

1.1 *Presentation*

When water flows over a spillway there is a region of clear water with a growing boundary layer and when this reaches the free surface the turbulence in the boundary layer can initiate natural air entrainment. If the air from the free surface does not reach the spillway surfaces the irregularities on the spillway surfaces will in a high speed flow cause small areas of flow separation and in these regions the pressure will be lowered and if the velocities are high enough the pressure may fall to below the local vapor pressure of the water and vapor bubbles will form. When these are carried downstream into high pressure region the bubble collapses giving rise to high pressures and possible cavitation damage.
Experimental investigations show that the damage can start at clear water velocities of between

Revision received February 6, 1989. Open for discussion till March 31, 1990.

12 to 15 m/s and up to velocities of 20 m/s it may be possible to protect the surfaces by streamlining the boundaries, improving the surface finishes or using resistant materials (Volkart and Rutschmann 1984) [1]. When air is present in the water the resulting mixture is compressible and this damps the high pressure caused by the bubble collapses (Peterka, 1953) [2]. If the velocities near the spillway bottom are sufficiently high, aerators must be introduced to prevent cavitation.

1.2 *Definitions*

The local air concentration C is defined as the volume of air per unit volume and this will normally be taken as a time averaged value. We define the characteristic depth d as:

$$d = \int_0^{Y_{90}} (1 - C) * dy \tag{1}$$

where y is measured perpendicular to the spillway surface. It is also necessary to define a characteristic depth for self aerated flow. For both model and prototype measurements a depth that is well defined and convenient is that where the average air concentration is 90% (Y_{90}).
A depth averaged mean air concentration for the flowing fluid can be defined from:

$$(1 - C_{mean}) * Y_{90} = d \tag{2}$$

An average water velocity is then:

$$U_w = \frac{q_w}{d} \tag{3}$$

The water discharge per unit width may be transformed:

$$q_w = (1 - C_{mean}) * U_w * Y_{90} \tag{4}$$

A characteristic water velocity (V_{90}) is defined as that at Y_{90}.

1.3 *Experiments*

The author (Chanson, 1988) [3] performed experiments on a 1 : 15 scale model of the Clyde dam spillway with a slope $\alpha = 52.33°$. The model provided Froude numbers in the range 3 to 25 with initial average flow velocities from 3 m/s to 14 m/s. By adjusting the gate at the entry of the flume the initial flow depth was from 20 mm to 120 mm. The first aerator configuration included a ramp of 5.7° (30 mm height, 300 mm length) and an offset of 30 mm height. This geometry was the same as that used by Low (1986) [4]. The second configuration had no ramp and an offset of 30 mm height as that used by Tan (1984) [5].
New conductivity probes were developed to record air concentration measurements with a single tip probe and velocity measurements of air-water mixture using a two-tips velocity probe and a cross-correlation probe.
In the first part the influence of air on cavitation and the main aerator devices are discussed. Then the data of Straub and Anderson (1958) [6] and Cain (1978) [7] in the aerated flow region are analyzed using the same method as that used by Wood (1985) [8]. Corrections are made to some of the coefficients calculated by Wood (1985) and there is some extension of his work. The third part deals with the gradually varied flow region downstream of an aerator (Fig. 1a) using the same method as that developed by Wood (1985) for the gradually varied flow region downstream of the

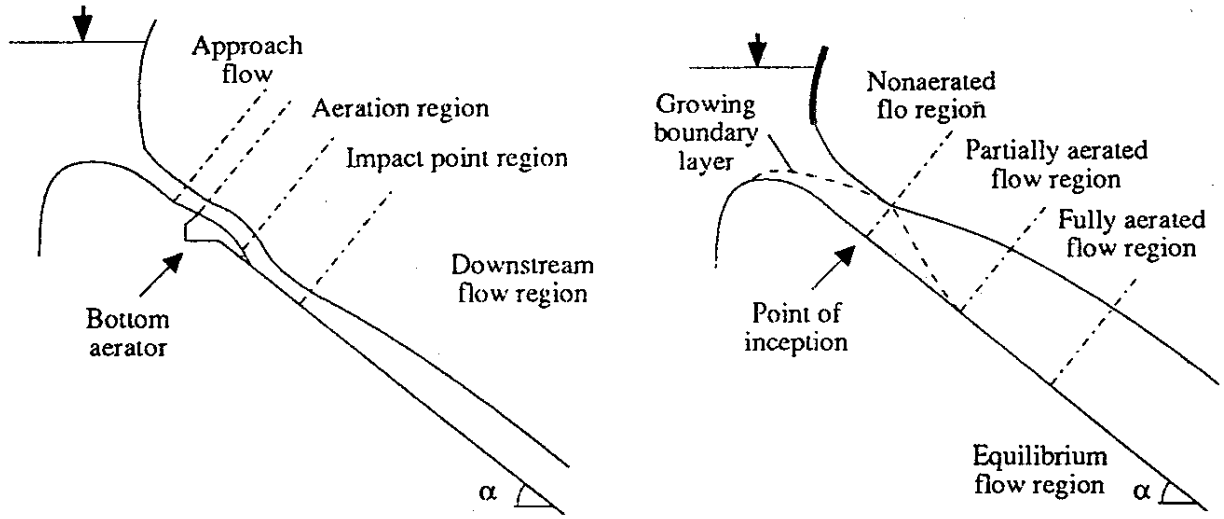

a b

Fig. 1. The major flows regions.
a. Spillway with bottom aerator
b. Open channel spillway

Les régions principales d'écoulement.
a. Evacuateur de crues équipé d'un aérateur de fond
b. Evacuateur de crue de surface

point of inception (Fig. 1b). In the fourth part the application of these results are developed and a method for aerator spacing is proposed.

2 Cavitation and aeration

2.1 *Effects of air on cavitation*

Russell and Sheehan (1974) [9] suggest that entrained air is effective because:

1. if there is any air present in the vapour cavities it will cushion the cavity collapse and reduce the resulting water hammer pressure (Hickling and Plesset, 1964) [10];
2. the presence of air bubbles in the water will reduce the celerity of the shock wave, and hence the magnitude of the shock waves on the material surface.

Peterka (1953) and Russell and Sheehan (1974) performed experiments on concrete specimens and showed that air concentrations of 1–2% reduce substantially the cavitation erosion and above 5–7% no erosion was observed.

On the boundary surface the local free air concentration is zero. Indeed the shear stress applied to an air bubble at the surface would split it in micro bubbles of negligible volume. Air concentration distributions on prototype (Cain, 1978) and scale model (Chanson, 1988) are plotted in Fig. 2 in comparison with the computed equilibrium profiles (detailed later). The results may be interpreted to indicate the presence of an air concentration boundary layer of about 10–15 mm near the spillway surface.

For particular conditions cavitation erosion will be reduced if the air concentration in the layers close to the bottom is above 1–2% and no damage will occur for air concentrations greater then 5–7%. In presence of a thick air concentration boundary layer, higher air concentrations may be required outside of that boundary layer.

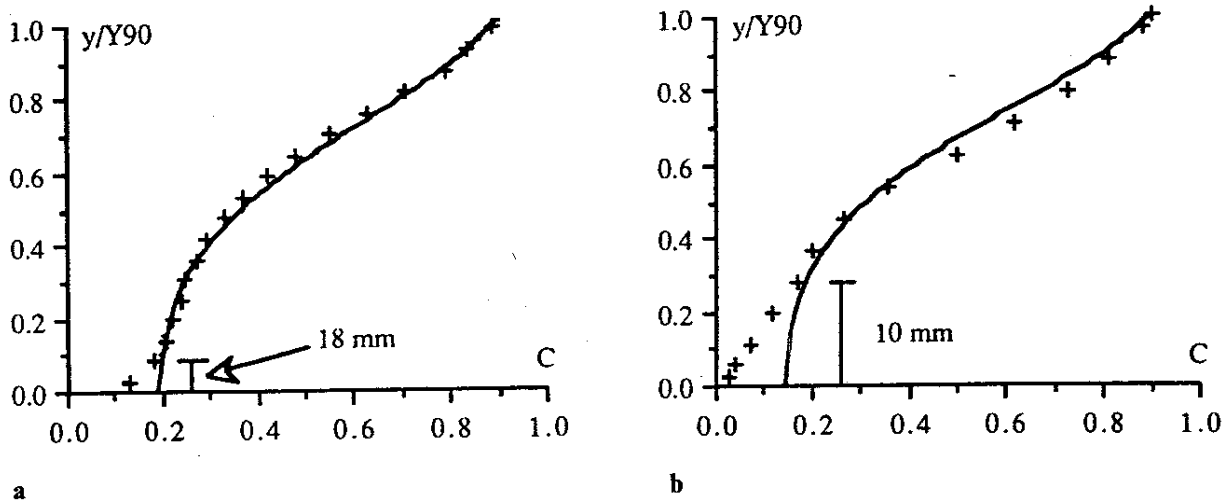

Fig. 2. Air concentration distribution near a spillway surface.
a. Aviemore data - Cain (1978)
b. Spillway model - Chanson (1988)

Profil de concentration en air près de la surface d'un évacuateur de crues.
a. Mesures à Aviemore - Cain (1978)
b. Modèle d'évacuateur de crues - Chanson (1988)

2.2 *Application - aerator devices*

The entrained air through the free surface of the flow may protect the spillway floor from cavitation damage if the free-surface aeration process provides a sufficient air concentration near the bottom (i.e. $C > 7\%$). If there is not enough surface aeration (i.e. downstream of a gate) or if the tolerances of surface finish required to avoid cavitation are too severe (i.e. $V > 30$ m/s), air can be artificially introduced by devices called aerators and located on the spillway floor and sometimes on the side walls.

A small deflection in a spillway structure (i.e. ramp, offset) tends to deflect the high velocity flow away from the spillway surface. In the cavity formed below the nappe, a local subpressure beneath the nappe (ΔP) is produced by which air is sucked into the flow (Q_{air}^{inlet}).

Vischer et al. (1982) [11] detailed the properties of the different types of aeration devices. Usually a combination of a ramp (slope ϕ), an offset (height t_s) and a groove provides the best design: the ramp dominates operation at small discharges while the groove provides space for the air supply and the offset enlarges the trajectory of the jet at higher discharges.

Table 1. Flow conditions at the end of the impact region on the Clyde dam spillway model - offset height: $t_s = 30$ mm
Conditions d'écoulement à la fin de la zone d'impact, sur le modèle de l'évacuateur de crues du barrage de Clyde - hauteur du décallage: $t_s = 30$ mm

initial depth d_0/t_s	mean air concentration C_*	reference depth d_*/t_s	slope α	conditions	reference
0.77	0.32	0.87	52.33°	no ramp	Chanson (1988)
1.15	0.26	1.10	52.33°	no ramp	Chanson (1988)
2.70	0.12	2.10	52.33°	no ramp	Chanson (1988)
1.67	0.29	1.15	51.30°	ramp $\phi = 5.7°$	Low (1986)

Volkart and Chervet (1983) [12] have studied on model the behaviour of a large range of aerators and Volkart and Rutschmann (1984) present several examples of air supply system.
The results obtained on the Clyde dam spillway model (Low, 1986, Chanson, 1988) indicate that the flow conditions at the start of the downstream flow region (reference depth d_*, mean air concentration C_*) are almost independent of the flow discharge, the subpressure ΔP in the cavity and the air flow provided by the air supply system Q_{air}^{inlet} (Table 1). These conditions are only function of the depth of water d_0 in the approach flow region of the aerator and the position of the start of the downstream flow region is a function of the position of the impact point of the jet. The latter is calculated from the jet trajectory equations, where the subpressure ΔP in the cavity is obtained from the air demand through the air inlets.

3 The equilibrium flow region

3.1 *Air Concentration Distribution*

Straub and Anderson (1958) published the classic set of aerated flow measurements in the uniform flow region. The re-analysis of their results by Wood (1985) shows that the depth averaged mean air concentrations C_{mean} (equation (2)) computed from Straub and Anderson's results is independent of the discharge and is a function of the slope only (Table 2).
The analysis of the continuity equation for the air phase (Wood, 1984) [13] gives the shape of the equilibrium air concentration distribution $C = f(y)$ for all mean air concentration value C_e:

$$C = \frac{B'}{B' + e^{-(G' * \cos \alpha * y'^2)}} \tag{5}$$

where y' is the non dimensional depth ($y' = y/Y_{90}$) and where B' and G' are constants only function of C_e (Table 2).

Table 2. Dimensionless air distribution - Straub and Anderson (1958)
Distribution adimensionnelle d'air - Straub et Anderson (1958)

slope	C_e	$G' * \cos \alpha$	B'
7.5°	0.161	7.99952	0.00302
15.0°	0.241	5.74469	0.02880
22.5°	0.310	4.83428	0.07157
30.0°	0.410	3.82506	0.19635
37.5°	0.569	2.67484	0.62026
45.0°	0.622	2.40096	0.81568
60.0°	0.680	1.89421	1.35393
75.0°	0.721	1.57440	1.86418

3.2 *The friction factor*

It was suggested earlier that:
1. the air concentration C is zero at the spillway surface;
2. there is an air concentration boundary layer.
However the boundary layer of air concentration does not coincide with the velocity boundary layer and the presence of air within the velocity boundary layer must be expected to reduce the shear stress between the flow layers and hence the value of the friction factor f.

Indeed for the spillway flow far downstream in the equilibrium region if the air concentration distribution is characterized by the mean air concentration C_e then it should be expected (Wood 1984) that:

$$f_e = \phi\left[\frac{d_e}{k_s}, Re, C_e\right] \tag{6}$$

where f_e is the friction factor for the equilibrium flow:

$$f_e = \frac{8 * g * \sin\alpha * d_e^3}{q_w^2},$$

α is the spillway slope, d_e is the equilibrium depth, k_s is the roughness and q_w is the water discharge per unit width.

If the variations in d_e/k_s are ignored, f_e calculated from Straub and Anderson's (1958) classic data decreases when the average air concentration C_e increases. It is interesting to note that until the mean air concentration reaches 20% there is no departure from the clear water value of f. At this stage the air concentration near the spillway floor is only of the order of 5%. There is at present no direct information about the way in which f_e varies with the roughness.

The equation (6) may be rewritten using the friction factor f in the non aerated flow as:

$$\frac{f_e}{f} = \phi_2[C_e] \tag{7}$$

3.3 *The velocity distribution*

Cain (1978) performed measurements of the velocity of the air-water interfaces in the aerated flow on Aviemore dam. His results which are consistent with those obtained by Keller et al. (1975) [14], are remarkable in that the velocity distribution may be written in the form suggested by Wood (1985) as (Chanson, 1988):

$$\frac{V}{V_{90}} = \left[\frac{y}{Y_{90}}\right]^{1/6} \tag{8}$$

It must be noted that the exponent was recalculated by the author and differs from the results of Wood (1985).

The experimental points on which this result depends were obtained for curves with a mean air concentration in the range 0 to 50%. It is therefore apparent that to an engineering approximation the velocity distribution is independent of the air concentration. This is based on the flow in the developing region. Since the distribution does not depend on the mean air concentration it is reasonable to expect that it will also apply to the uniform flow region (Wood, 1985) and this enables all the properties in this region to be estimated.

The characteristic velocity V_{90} defined as that for Y_{90} is deduced by combining the equation (8) with the continuity equation for the water phase (Chanson, 1988):

$$V_{90} = \frac{q_w * Y_{90}^{1/6}}{\int_0^{Y_{90}} (1 - C) * y^{1/6} * dy} \tag{9}$$

where C is computed from the equation (5) and Y_{90} is obtained from the equation (2).

3.4 *Flow parameters*

As detailed by Wood (1985), for any spillway slope the Table 2 gives a reasonable estimate of the equilibrium air concentration C_e. If the value of the friction factor f in the non aerated flow is available then the equation (7) gives the friction factor f_e in the air entrained flow. This enables the reference depth d_e to be computed from:

$$d_e = \left[\frac{q_w^2 * f_e}{8 * g * \sin \alpha} \right]^{1/3} \tag{10}$$

Knowing C_e and d_e the average water velocity U_w and Y_{90} are obtained from equations (3) and (2). The air concentration distribution is computed from the equation (5) and the water velocity distribution is obtained from the equations (8) and (9).

4 Flow region downstream of an aerator

4.1 *Introduction*

Wood (1985) showed that, for: {H1} a slow rate of air entrainment, {H2} a quasi-hydrostatic pressure distribution, and {H3} slow variations of the velocity, the continuity equation for the air phase and the energy equation provide two differential equations in terms of the flow depth d and the mean air concentration C_{mean} at any section in the gradually varied flow region downstream of the point of inception (Fig. 1b).

If the assumptions H1, H2 and H3 are respected, Chanson (1988) showed that the equations developed by Wood (1985) can be applied in the flow region downstream of an aerator. Firstly the equations will be presented and then applied to the downstream flow region. The results are later used to define a method for aerator location and aerator spacing.

4.2 *The entrainment function*

On a spillway downstream of an aerator we consider the flow region far enough downstream of the impact point of the water jet. In this region the graphs of the quantity of air entrained within the flow (Chanson, 1988) show a slow rate of entrainment. This suggests that for a given mean air concentration $C_{mean}(x)$ the air concentration distribution will have a shape that is close to the equilibrium air concentration. The comparison of the shapes of the air concentration curves for the author's measurements in the flow region downstream of an aerator with the equilibrium profile (equation (5)) illustrates this point (Fig. 3).

Cain's (1978) velocity measurements were performed in the developing region and it seems therefore that, in any gradually varied flow region, such a velocity distribution (equations (8) and (9)) will hold. The author observed similar velocity distribution downstream of an aerator as that obtained by Cain. The dimensionless plot is presented in Fig. 4 where V_{90} is calculated from the equation (9) and the data are compared with the power law (equation (8)). The scatter of these points differs from the results of Cain (1978) because of the limitation of the instrumentation on spillway model.

With the same method as that used by Wood (1985) the continuity equation for air downstream of an aerator is:

$$\frac{d}{dx} q_{air} = V_e(x) - C_{mean}(x) * u_r * \cos \alpha \tag{11}$$

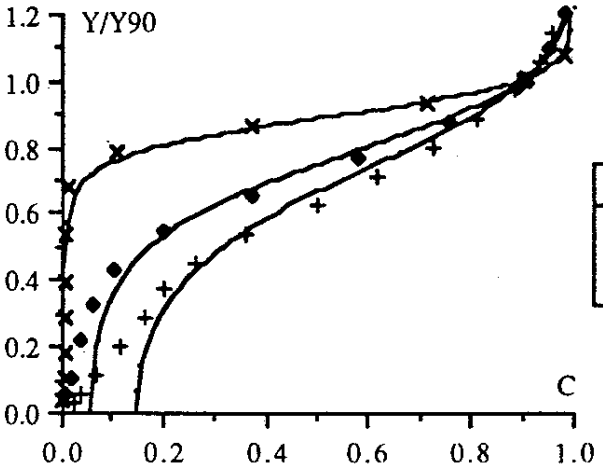

	Ref.	qw	Cmean	d
+	860-1	0.2118	0.3952	0.0212
◆	873-1	0.2731	0.2957	0.0258
×	880-1	0.4291	0.1203	0.0491

Fig. 3. Comparison of the author's data with the equilibrium air concentration profile.
Comparaison des mesures de l'auteur avec le profil théorique d'équilibre.

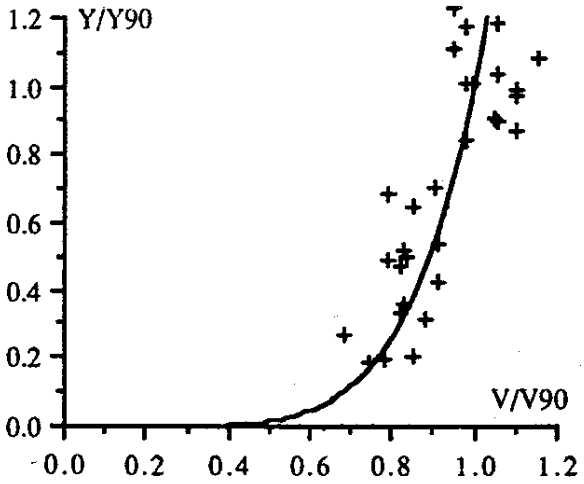

Fig. 4. Velocity distribution downstream of an aerator on spillway model - Chanson (1988).
Profil des vitesses en aval d'un aérateur de fond, mesurées sur modèle - Chanson (1988).

where V_e is the local entrainment velocity (Wood 1985), C_{mean} is the local average air concentration, u_r is the rise bubble velocity in the downstream flow region and α is the spillway slope. Using the limit of the equation (11) in the equilibrium flow region:

$$0 = \{V_e\}_e - C_e * u_r * \cos \alpha$$

the continuity equation (11) yields:

$$\frac{d}{dx} q_{air} = (V_e(x) - \{V_e\}_e) + (C_e - C_{mean}(x)) * u_r * \cos \alpha \quad (12)$$

Wood (1985) proposes to neglect the first term in the equation (12) and this equation then becomes:

$$\frac{d}{dx} q_{air} = C_e * u_r * \cos \alpha - C_{mean} * u_r * \cos \alpha$$

This is equivalent to assuming that for a gradually varied flow region the rate of entrainment is a constant and equal to the equilibrium rate of entrainment but the rate of escape of air is proportional to the local air concentration.
The quantity of air entrained may be rewritten (Chanson, 1988):

$$q_{air} = \frac{C_{mean}}{1 - C_{mean}} * q_w$$

With these approximations the continuity equation for the air phase becomes:

$$\frac{d}{dx} C_{mean} = \frac{u_r * \cos \alpha}{q_w} * (C_e - C_{mean}) * (1 - C_{mean})^2 \tag{13}$$

and integrating the above yields:

$$\frac{1}{(1 - C_e)^2} * \text{Ln}\left[\frac{1 - C_{mean}}{C_e - C_{mean}}\right] - \frac{1}{(1 - C_e) * (1 - C_{mean})} = k * x + K_0 \tag{14}$$

where K_0 is the integration constant. For the flow downstream of an aerator the initial conditions are taken at the start of the downstream flow region. Thus K_0 is computed for $C_{mean} = C_*$ at $x = 0$:

$$K_0 = \frac{1}{(1 - C_e)} * \left[\frac{1}{(1 - C_e)} * \text{Ln}\left[\frac{1 - C_*}{C_e - C_*}\right] - \frac{1}{(1 - C_*)}\right]$$

and

$$k = \frac{u_r * \cos \alpha}{q_w}$$

Cain's (1978) data on Aviemore and the author's data on spillway model were used to check the above relationship (Chanson, 1988). For two discharges Cain's data give two straight lines with a correlation higher than 0.95 and imply values of u_r of 40 cm/s. These values are close to the still water values published in COMOLET (1979) [15].
On spillway model the data imply values of the rise bubble velocity u_r in the downstream flow region from 1 to 16 cm/s which is lower than those obtained from Aviemore's measurements. This may be explained by: 1. the high level of turbulence at the start of the downstream flow region; 2. the size of the air bubbles and its distribution.
For an annular jump Haindl (1969) [16] indicates that the ratio u_r^t/u_r may be as low as 0.25, where u_r^t is the terminal velocity of bubbles in turbulent flow and u_r the rise bubble velocity in still water. It must be remarked that the high turbulence level downstream of the impact region may slowly tend to drop. Far away downstream of the aerator the turbulence may reach similar intensity as that on open channel flow in the equilibrium flow region.
Comolet (1979) showed that the rise bubble velocity in still water may be rewritten:

$$u_r = \sqrt{\frac{2 * \Delta}{C_x} * d_b * g * \left(1 - \frac{\varrho_{air}}{\varrho_w}\right)} \tag{15}$$

where C_x is the drag coefficient, d_b the bubble size and Δ a shape coefficient

$$\left(\Delta = \frac{V}{s * d_b}\right).$$

The equation [15] indicates that the rise velocity is proportional to $\sqrt{d_b}$. The results obtained from Comolet (1979) and the data obtained on spillway model by the author are presented in Table 3 as a function of the average bubble size d_b.

The average rise bubble velocity is a function of the turbulence intensity and the bubble size distribution. This suggests that the results on spillway model may be affected by scale effects if these parameters are different from those on prototype.

If the distribution of the rise bubble velocity along the flume is known then the equation [14] may be integrated as:

$$\frac{1}{(1-C_e)^2} * \mathrm{Ln}\left[\frac{1-C_{mean}}{C_e-C_{mean}}\right] - \frac{1}{(1-C_e)*(1-C_{mean})} = \frac{\cos\alpha}{q_w} * \int_{x=0}^{x=L} u_r * dx$$

If the average rise bubble velocity u_r is assumed constant, the equation (14) gives the air concentration down the spillway as a function of x. Denoting $d = d_*$ at $x = 0$ the dimensionless relationship in term of $x' = x/d_*$ is then deduced:

$$\frac{d}{dx'} C_{mean} = \frac{u_r * \cos\alpha}{q_w} * (C_e - C_{mean}) * (1 - C_{mean})^2 * d_* \qquad (16)$$

where u_r and q_w are constant and C_e is function of α only. It must be emphasized that the equation (16) allows calculations of the average air concentration in function of the distance along the channel independently of the velocity, the roughness and the depth of water.

Table 3. The rise bubble velocity as a function of the bubble size
La vitesse d'ascension d'une bulle d'air en fonction des dimensions de la bulle d'air

d_b	u_r	remarks
1 mm	12 cm/s	spherical bubble in still water, Comolet (1979)
2 mm	24 cm/s	spherical bubble in still water, Comolet (1979)
4 mm	35 cm/s	spherical bubble in still water, Comolet (1979)
1 mm	1 cm/s	downstream flow region, Chanson (1988)
3.1 mm	11 cm/s	downstream flow region, Chanson (1988)

4.3 *The energy equation*

Wood (1985) developed the energy equation for a streamline at a depth y above the bed:

$$E(y) = \varrho(y) * g * (z + y * \cos\alpha) + \int_{y}^{\infty} \varrho(h) * g * \cos\alpha * dh + \varrho(y) * \frac{(u(y))^2}{2}$$

Assuming that: 1. the pressure distribution *is* quasi-hydrostatic and 2. the velocity distribution verifies:

$$q_w * d = \int_{0}^{Y_{90}} (1 - C) * y * V(y) * dy$$

the mean specific energy becomes:

$$SE = z + d * \cos\alpha + E * \frac{d}{2} * Fr^2 \qquad (17)$$

where

$$y' = \frac{y}{Y_{90}}, \qquad V' = \frac{V}{V_{90}}, \qquad Fr = \frac{U_w}{\sqrt{g * d_*}}$$

and the parameter E is defined as (Wood, 1985):

$$E = (1 - C_{mean})^2 * \frac{\int_0^1 (1 - C) * u'^2 * dy'}{\left[\int_0^1 (1 - C) * u' * dy'\right]^3} \tag{18}$$

The velocity distribution may be estimated from equation (8) and the parameter E becomes:

$$E = (1 - C_{mean})^2 * \frac{\int_0^1 (1 - C) * y'^{2/6} * dy'}{\left[\int_0^1 (1 - C) * y'^{1/6} * dy'\right]^3} \tag{19}$$

where C is computed from the equation (5). E is only function of the mean air concentration. Numerical computations of E are plotted in Fig. 5 and compared with data on Aviemore and on spillway model.

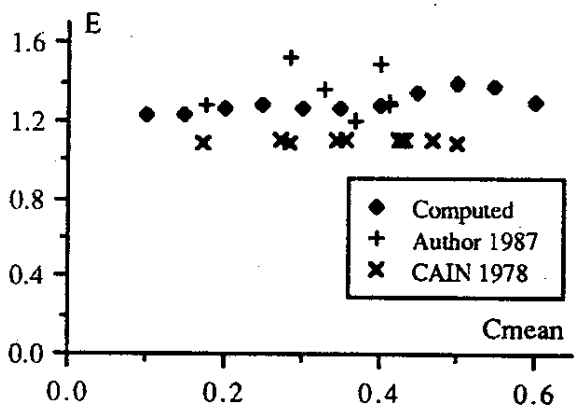

Fig. 5. Parameter E as function of the mean air concentration.
Paramètre E en fonction de la concentration en air moyenne.

For a spillway with gradually varied width and slope, and using the momentum equation:

$$\frac{d}{dx} SE = S_f$$

the equation (17) becomes:

$$\frac{d}{dx} d = \frac{\sin \alpha * \left(1 + d * \frac{d\alpha}{dx}\right) - S_f + \frac{E * d}{W} * Fr^2 * \frac{dW}{dx}}{\cos \alpha - E * Fr^2} \tag{20}$$

The slow growth of the aerated layer implies a local equilibrium and this suggests that the equilibrium friction factor may also be used with local rather than equilibrium values (Wood, 1985). The knowledge of S_f is obtained from equation (7):

$$S_f = \frac{q_w^2 * f}{8 * g * d^3} * \phi_2(C_{mean})$$

where the function ϕ_2 is defined in equation (7) (Wood, 1985).
The energy equation may be rewritten in term of

$$x' = \frac{x}{d_*}, \quad d' = \frac{d}{d_*}, \quad W' = \frac{W}{d_*} \quad \text{and} \quad Fr_* = \frac{q_w}{\sqrt{g * d_*^3}}$$

where $d = d_*$ at $x = 0$ and then becomes:

$$\frac{d}{dx'} d' = \frac{\sin \alpha * \left(1 + d' * \frac{d\alpha}{dx'}\right) - S_f + E * \frac{d'}{W'} * \frac{Fr_*^2}{d'^3} * \frac{dW'}{dx'}}{\cos \alpha - \frac{E * Fr_*^2}{d'^3}} \tag{21}$$

where the local values of S_f and E are function of C_{mean}.

4.4 *Application*

4.4.1 Introduction

The equations (16) and (21) provides two simultaneous differential equations in terms of the reference depth d and the average air concentration C_{mean} and these equations can be solved using numerical methods. The knowledge of d and C_{mean} at any point on the spillway leads to the calculations of the air concentration distribution (equation (5)) and the velocity distribution (equations (8) and (9)) at any point.
In the particular case a spillway with constant width the flow parameters d and C_{mean} are obtained from a simple system of equations:

$$\frac{d}{dx'} C_{mean} = \frac{u_r * \cos \alpha}{q_w} * (C_e - C_{mean}) * (1 - C_{mean})^2 * d_* \tag{22}$$

$$\frac{d}{dx'} d' = \frac{\sin \alpha * \left(1 + d' * \frac{d\alpha}{dx'}\right) - S_f}{\cos \alpha - \frac{E * Fr_*^2}{d'^3}} \tag{23}$$

which can be solved numerically. These equations were used to reproduce the air entrainment on spillway model (Chanson 1988). The results are presented in Fig. 6 where the origin is taken at the end of the deflector and the initial conditions were obtained from the Table 1.

4.4.2 The application of the proposed method to the Clyde dam spillway

The Clyde dam spillway (New Zealand) has a 70 m long steep spillway ($\alpha = 51.34°$ and $50.19°$) followed by a stilling basin (50 m long) with a 8 : 1 reverse slope which ends by a flip bucket (Fig. 7). The aerator is located 39 m below the reservoir flood level and 28 m above the stilling

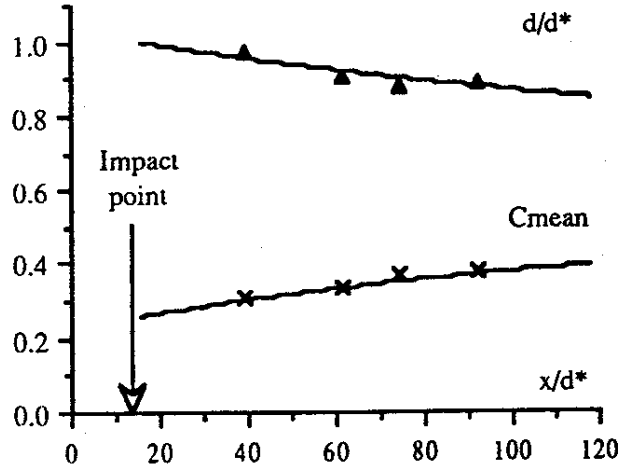

Fig. 6. Air concentration profiles at the point H, $q_w = 21$ m^3/s/m, $u_r = 40$ cm/s.
Profils de concentration en air au point H, $q_w = 21$ m^3/s/m, $u_r = 40$ cm/s.

basin invert. The position of the main characteristic points (Fig. 8) is reported in the Table 4 where S is the curviline coordinate from the point B.

The equations (22) and (23) determine the air entrainment on the spillway and on the stilling basin and hence it is possible to compare the air entrainment on the spillway with and without aerator. It must be remarked that the equation (23) was obtained for a hydrostatic pressure distribution. The transition F-G between the spillway and the stilling basin occurs with a circular turn ($R = 20$ m) and Henderson (1966) [17] shows that the increase of pressure due to the turn is small for $d/R > 10$ (i.e. for a depth of water d lower than 2 m). Hence the assumption of the hydrostatic pressure distribution is reasonable for $d < 2$ m.

For a water discharge $q_w = 21$ m^3/s/m the surface roughness $k_s = 3$ mm gives a friction factor $f = 0.025$. The only value of the rise bubble velocity on prototype is the result from Cain's (1978) data on Aviemore dam. This result ($u_r = 40$ cm/s) may be used for the flow downstream of the

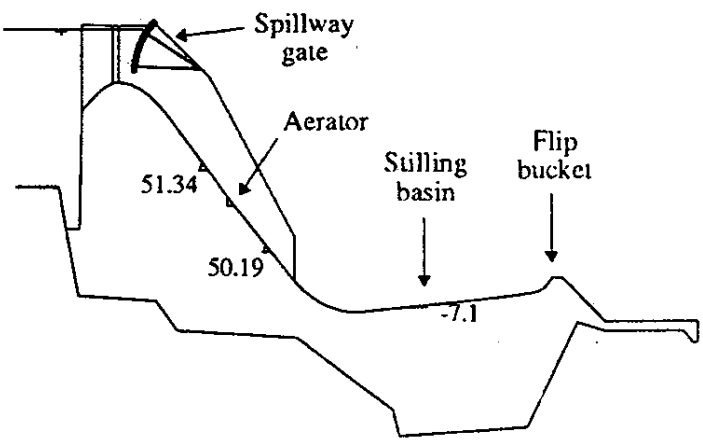

Fig. 7. Clyde dam spillway and stilling basin.
Evacuateur de crues du barrage de Clyde, avec le bassin de dissipation.

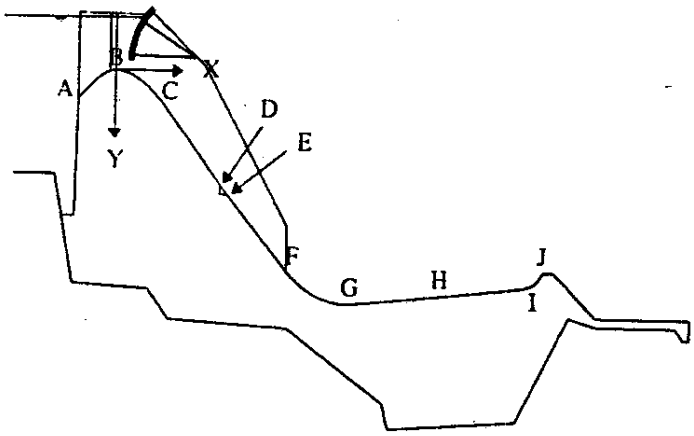

Fig. 8. Characteristic points of the spillway.
Point caractéristiques de l'évacuateur de crues.

point of inception (spillway without aerator). The extrapolation of the results obtained on spillway model may be affected by scale effects and hence for the flow downstream of the aerator the rise bubble velocity on prototype is taken as that on Aviemore dam ($u_r = 40$ cm/s).
For this water discharge and surface roughness the point of inception of air entrainment for the spillway without aerator was computed from Keller and Rastogi (1977) [18]. These calculations provide $S_I = 73$ m and $d_I = 0.675$ m where S_I is the curviline co-ordinate along the spillway surface from the origin B (Fig. 8) and d_I the flow depth. This position corresponds to the start of the turn at the end of the spillway (point F).
For a water discharge $q_w = 21$ m^3/s/m the water depth in the approach flow region of the aerator (point D) is $d_0 = 0.75$ m and the computed impact point of the jet (Chanson 1988) is located 13.5 m downstream of the end of the deflector. Assuming that the downstream flow region starts 18.5 m downstream of the end of the deflector, the initial air concentration C_* and flow depth d_* are estimated from the results on spillway model (Table 1): $C_* = 0.26$ and $d_* = 0.72$ m.
The results are summarized in the Table 5 for this particular discharge. At the position H in the middle of the stilling basin the air concentration profiles are plotted in Fig. 9 for the cases: 1. without aerator and 2. with the aerator (at the point D).
The results (Fig. 9) suggest that without aerator cavitation would occur on the spillway and on the stilling basin because the air concentration near the spillway bottom is below the required minimum to prevent cavitation damage. For this particular discharge the presence of the aerator (at the position D) should prevent cavitation erosion on the spillway and for most of the stilling basin but damage may occur at the end of the stilling basin (between H and I) as the air concentration in the layer close to the spillway surface ($C = 2$-3%) is below the required minimum 5-7%.
It must be emphasized that these results depend critically on the assumed rise bubble velocity u_r, the friction factor f, the initial air concentration C_*, the initial flow depth d_*. It is worth noting that the greatest uncertainty applies on the assumed rise bubble velocity u_r.

4.5 *Aerator spacing*

4.5.1 Presentation

Air concentration downstream of an aerator and in the layer close to the spillway surface is of primary importance for cavitation erosion protection. In the impact point region the turbulence

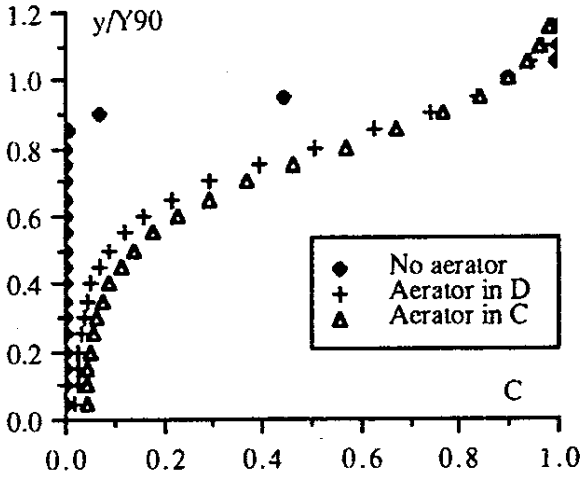

Fig. 9. Air entrainment on spillway model, $q_w = 0.40$ m^3/s/m, $d_0/t_s = 1.15$, $u_r = 16$ cm/s, $d_* = 0.039$ m, $C_* = 26\%$.

Entraînement d'air sur modèle, $q_w = 0{,}40$ m^3/s/m, $d_0/t_s = 1{,}15$, $u_r = 16$ cm/s, $d_* = 0{,}039$ m, $C_* = 26\%$.

Table 4. Clyde dam spillway - characteristic points
Evacuateur de crues du barrage de Clyde - points caractéristiques

point	elevation (m)	Y (m)	X (m)	α	S (m)	remark
A		6.90	- 8.50	-45.0°	-11.2	
B	182.00	0.00	0.00	0.00°	0.00	origin point
C	172.16	9.84	14.00	51.34°	17.53	
D		26.15	27.06	51.34°	38.42	end of the offset
E	153.00	29.00	28.75	50.19°	41.74	end of the groove
F	135.20	46.80	43.59	50.19°	64.91	end of spillway start of circular turn: $R = 20$ m
G		54.11	62.09	- 7.125°	85.65	end of turn start of stilling basin
H		51.71	81.28	- 7.125°	105.00	
I		49.01	102.85	- 7.125°	126.73	end of stilling basin start of circular turn: $R = 1.48$ m
J	137.00	45.00	111.07	-68.20°	135.93	end of flip bucket

Table 5. Results for $q_w = 21$ m^3/s/m and $u_r = 40$ cm/s
Résultats pour $q_w = 21$ m^3/s/m et $u_r = 40$ cm/s

point	S (m)	α	d (m) without aerator	C_m	d (m) aerator in D	C_m	d (m) aerator in C	C_m	remark
	30.13	51.34°					1.43	0.26	start of the downstream flow region
	56.92	50.19°			0.720	0.26			start of the downstream flow region
F	64.91	50.19°	0.675	0.00	0.701	0.28	0.878	0.33	end of spillway
G	85.65	- 7.125°	0.687	0.07	0.710	0.28	0.851	0.32	start of stilling basin
H	105.00	- 7.125°	0.750	0.05	0.774	0.23	0.928	0.27	
I	126.73	- 7.125°	0.826	0.04	0.853	0.17	1.026	0.21	end of stilling basin
J	135.93	-68.20°	0.903	0.03	0.938	0.16	1.157	0.19	end of flip bucket

in the flow redistributes the air bubbles. The air concentration distribution in the downstream flow region tends to the equilibrium distribution of the particular slope and this can be estimated from the equations (16) and (21).
The spillway surface will not be protected from cavitation erosion when the air concentration near the spillway floor falls below a minimum amount of 5 to 10% and this means an average air concentration C_{mean} below 30% (Table 2).
On a steep spillway ($\alpha > 20°$) the air concentration distribution downstream of an aerator will tend to the equilibrium air concentration distribution where $C_e > 30\%$ (Table 2). If the average air concentration at the start of the downstream flow region is high enough ($C_{mean} > 25$–30%) all the length downstream of the first aerator will be protected and no additional aerator will be required as long as $\alpha > 20°$. If the spillway slope becomes lower than 20° or for a flat spillway ($\alpha < 20°$) the flow may be de-aerated and an additional aerator will be required when the average air concentration C_{mean} becomes lower than 30%.

4.5.2 Application

A bottom aerator introduces artificially a large quantity of air in the flow over a short distance and the quantity of air entrained is function of the characteristics of the aerator (Table 1).
For a flat spillway the flow is de-aerated downstream of an aerator and the first aerator must be located immediately upstream of the start of cavitation. For a steep spillway the first aerator must be positioned as upstream as possible to combine the effects of 1. the artificial aeration of the aerator and 2. the natural free surface aeration downstream of the aerator.
For the Clyde dam spillway the effect of a virtual location of the aerator at the point C was studied (Table 5). For the particular discharge $q_w = 21$ m^3/s/m as previously described, the flow depth upstream of the aerator (in C) would be $d_0 = 1.5$ m and the impact point, computed from Chanson (1988), would be located 8.4 m downstream of the point C. Assuming that the downstream flow region would start 12.6 m downstream of the point C, the initial air concentration C_* and flow depth d_* are estimated from the Table 1: $C_* = 0.26$ and $d_* = 0.72$ m.
The results (Table 5) show a stronger flow aeration. The air concentration at the middle of the stilling basin (point H) is presented in Fig. 9. The comparison with the previous results (without aerator and aerator in D) indicates that the local air concentration, at the point H, and at 20 mm from the spillway surface (equation (5)), would be: $C = 0\%$ without aerator, $C = 2\%$ with the aerator in D and $C = 4\%$ with the aerator in C.

5 Conclusion

A complete analogy between the flow downstream of an aerator and the flow on a free-surface aerated spillway has been developed. In the gradually varied flow region a simple analysis (Wood 1985) based on the continuity equation and the energy equation provides two simultaneous differential equations which can be solved by numerical method and reproduce air entrainment on a spillway. The same equations may be derived in the flow downstream of an aerator.
Predictions of air entrainment downstream of an aerator can be computed by this method and this provides a satisfactory method to calculate the aerator spacing.
It must be emphasized that the estimation of the rise bubble velocity in the downstream flow region requires additional prototype measurements.

6 Acknowledgements

The author wishes to thank the Civil Engineering Department, University of Canterbury (New Zealand), the University Grant Committee (New Zealand) and the Ministry of Works and Development (New Zealand) for their financial support, and Professor I. R. Wood who supervised with project.

Notations

B' integration constant of the equilibrium air concentration distribution
C air concentration defined as the volume of air per unit volume
C_e depth averaged equilibrium air concentration
C_{mean} depth averaged mean air concentration defined as: $(1 - C_{mean}) * Y_{90} = d$
C_* mean air concentration at the start of the downstream flow region
d characteristi depth (m) defined as:

$$d = \int_0^{Y_{90}} (1 - C) * dy$$

where y is measured perpendicular to the spillway surface
d_e equilibrium flow depth (m)
d_I flow depth at the inception point (m)
d_0 characteristic depth in the approach flow region
d_* characteristic depth (m) at the start of the downstream flow region
d' dimensionless characteristic depth
Fr Froude number defined as:

$$Fr = \frac{V}{\sqrt{g * d}}$$

f friction factor
f_e friction factor of the equilibrium flow
G' integration constant of the equilibrium air concentration distribution
g gravity constant (m/s^2)
local value: $g = 9.8050$ m/s^2 (Christchurch, New Zealand)
k_s equivalent uniform roughness (m)
L_{is} distance along the spillway from the point of inception (m)
L_{jet} distance of the impact point of the jet from the end of the deflector (m)
L_{ramp} ramp length (m)
P_{atm} atmospheric pressure above the flow (Pa)
P_{cavity} absolute pressure in the cavity (Pa)
P_0 absolute pressure above the flow (Pa)
Q_{air}^{inlet} air discharge provided by the air supply system (m^3/s/m)
Q_w water discharge (m^3/s)
q_{air} quantity of air entrained within the flow per unit width (m^3/s/m)
q_w water discharge per unit width (m^3/s/m)
S curviline co-ordinate (m)
SE mean specific energy (m)
t_s offset height (m)

U_w average water velocity (m/s) defined as: $U_w = \frac{q_w}{d}$
u local velocity (m/s)
u_r rise bubble velocity (m/s)
V velocity (m/s)
V_{90} characteristic velocity at Y_{90} (m/s)
W channel width (m)
W' dimensionless width
x distance from the end of the deflector (m)
x' dimensionless distance
Y_{90} characteristic depth (m) where the air concentration is 90%
α spillway slope
ΔP difference between the pressure above the flow and the air pressure beneath the nappe (Pa): $\Delta P = P_0 - P_{cavity}$
ϕ angle between the ramp and the spillway
ϱ_{air} density of air (kg/m^3)
ϱ_w density of water (kg/m^3)

References / Bibliographie

1. VOLKART, P. and RUTSCHMANN, P., Air Entrainment Devices, Mitteilungen der Versuchsanstalt für Wasserbau, Hydrologie und Gaziologie, No. 72, Zürich, Switzerland, 1984.
2. PETERKA, A. J., The Effect of Entrained Air on Cavitation Pitting, Joint meeting paper, IAHR/ASCE, Minneapolis, USA, August 1953.
3. CHANSON, H., Study of Air Entrainment and Aeration Devices on Spillway Model, Research Report 88-8, University of Canterbury, New Zealand, October 1988.
4. LOW, H. S., Model Studies of Clyde Dam Spillway Aerators, Master Report, Ref. 86-8, University of Canterbury, New Zealand, 1986.
5. TAN, T. P., Model Studies of Aerators on Spillway, Master Report, Ref. 84-6, University of Canterbury, New Zealand, 1984.
6. STRAUB, L. G. and ANDERSON, A. G., Experiments on Self-Aerated Flow in Open Channel, J. of Hyd. Div., ASCE, Vol. 84, HY7, 1958.
7. CAIN, P., Measurements within Self-Aerated Flow on a Large Spillway, Ph.D. Thesis, Ref. 78-18, University of Canterbury, Christchurch, New Zealand, 1978.
8. WOOD, I. R., Air Water Flows, 21st Congress IAHR, August 1985, Melbourne, Australia.
9. RUSSELL, S. O. and SHEENAN, G. J., Effect of Entrained Air on Cavitation Damage, Canadian Journal of Civil Engineering, Vol. 1, 1974.
10. HICKLING, R. and PLESSET, M. S., Collapse and Rebound of a Spherical Bubble in Water, The Physics of Fluids, Vol. 7, No. 1, January 1964, pp. 7–14.
11. VISCHER, D., VOLKART, P. and SIGENTHALER, A., Hydraulic Modelling of Air Slots on Open Chute Spillways, Int. Conf. on Hydraulic Modelling, BHRA Fluid Engineering, Coventry, England, September 1982.
12. VOLKART, P. and CHERVET, A., Air Slots for Flow Aeration, Mitteilungen der Versuchsanstalt für Wasserbau, Hydrologie und Glaziologie, No. 66, Zürich, Switzerland, 1983.
13. WOOD, I. R., Air Entrainment in High Speed Flows, Symp. on Scale Effects in Modelling Structures, IAHR, Esslingen, 1984.
14. KELLER, R. J., LAI, K. K. and WOOD, I. R., Developing Region in Self-Aerated Flow, J. of Hyd. Div., ASCE, Vol. 101, HY9, Proc. Paper 10501, April 1974, pp. 553–568.
15. COMOLET, R., Sur le Mouvement d'une bulle de gaz dans un liquide (Gas bubble motion in a liquid medium), La Houille Blanche, No. 1, 1979, pp. 31–42.
16. HAINDL, K., Zone Lengths of Air Emulsion in Water Downstream of the Ring Jump in Pipes, 13th Congress IAHR, August 1969, Vol. 2, pp. 9–19, Kyoto, Japan.
17. HENDERSON, F. M., Open Channel Flow, MacMillan Company, New York, 1966.
18. KELLER, R. J. and RASTOGI, A. K., Design Chart for Predicting Critical Point on Spillways, J. of Hyd. Div., ASCE, HY12, Proc. Paper 13426, December 1977, pp. 1417–1429.